

11-15-2013

Simulation of Vertical Axis Wind Turbines With Variable Pitch Foils

L. Damon Woods
Boise State University

John F. Gardner
Boise State University

Kurt S. Myers
Idaho National Laboratory

IMECE2013-65694

SIMULATION OF VERTICAL AXIS WIND TURBINES WITH VARIABLE PITCH FOILS

L. Damon Woods
Boise State University
Boise, ID, USA

John F. Gardner
Boise State University
Boise, ID, USA

Kurt S. Myers
Idaho National Laboratory
Idaho Falls, ID, USA

ABSTRACT

A dynamic computer model of a turbine was developed in MATLAB in order to study the behavior of vertical axis wind turbines (VAWTs) with variable pitch (articulating) foils. The simulation results corroborated the findings of several empirical studies on VAWTs. The model was used to analyze theories of pitch articulation and to inform the discussion on turbine design. Simulations of various models showed that pitch articulation allowed Darrieus-style vertical axis wind turbines to start from rest. Once in motion, the rotor was found to accelerate rapidly to very high rotational velocities. The simulations revealed a plateau region of high efficiency for small-scale Darrieus-style VAWTs with symmetric airfoils at tip speed ratios in the range of 3 to 4 and demonstrated the advantages of using a dynamic generator load.

NOMENCLATURE

A = Area of flow intercepted by the turbine
 a = Induction factor
 C = Chord length
 C_d = Coefficient of drag
 C_l = Coefficient of lift
 C_p = Coefficient of power
D = Drag force
H = Span
L = Lift force
P = Power
R = Radius
Re = Reynolds number
TSR = Tip speed ratio

U = Free-stream velocity of the fluid
 U_{tot} = Magnitude of the total flow velocity
VAWT = Vertical axis wind turbine
 α = Angle of attack
 θ = Rotor position
 μ = Viscosity
 Π = Geometric transform
 ρ = density of the fluid
 τ = Torque
 ω = Rotational velocity

INTRODUCTION

Thousands of wind turbines are currently employed in the production of electricity. In 2010 alone over 37,000 Megawatts of new wind power-generating capacity were installed worldwide [1], and many experts predict that wind could make up to 20% of the U.S. electricity needs by the year 2030 [2]. In 2011 wind accounted for 3% of the electricity consumed for U.S. [3].

Harnessing the elements to do useful work is nothing new. There are records of windmills installed in Persia dating back to 200 BC [4]. What has changed over the centuries is how effectively people are able to make use of these vast energy resources. Sophisticated computer models can now be developed based on the physics of the turbines. A computer model that predicts the performance of new design iterations can streamline the design process which used to rely on physical experimentation of each new design that is both costly and time consuming.

This particular study was motivated by a novel design of a VAWT with articulated foils and improved start-up behavior. The purpose of the model is to inform both the mechanical design and the real-time control of the turbine to maximize performance and improve mechanical design.

BACKGROUND

Although most wind energy today comes from large, three-bladed horizontal axis wind turbines, a niche market has emerged for smaller Vertical Axis Wind Turbines (VAWTs) [5]. VAWTs can operate with wind coming from any direction and can operate in harsher wind conditions (lower wind-speeds, more turbulence) than HAWTs [6]. These turbines are sometimes installed on building roofs as a way of capturing energy in windy urban areas providing distributed power generation and can be used to gain Leadership in Energy Efficient Design (LEED) credits for a building. LEED is a metric for the sustainability and environmental friendliness of a structure.

One of the motivations for this study was a new patent for a VAWT with articulating foils known as the BlackHawk TR-10 [7]. This turbine used a novel variable pitch system to enable it to start from rest without any external inputs – something traditional VAWTs have had issue with for years [8]. Traditional VAWTs act as a power *draw* before they can act as a power *source*, putting additional strain on the grid. Conventional gas turbines face the same problem.

By creating a means by which the foils change their pitch as a function of rotor angle, they are able to present their foils to the wind at an angle of attack (α) that increases torque to the rotor. Ideally, turbines would be able to articulate their foils to catch the best angle at every point in their rotation around the axis in order to maximize their torque. One researcher who has explored this theory [9] posits three ideal examples of turbine articulation. The first concept is to keep α at slightly less than the local stall angle, ensuring maximum lift. Unfortunately, this concept cannot be realized in a physical environment because the ideal pitch function has two step changes of the pitch angle during the rotation. These sudden changes in foil angles are problematic from a mechanical design perspective and could prove disastrous to a mechanical turbine at high speeds. A second concept proposed a slightly more gradual adjustment at these points, but pitch angle changes required were still too sudden to avoid mechanical failure. The third concept for increasing efficiency through pitch articulation is to vary the pitch sinusoidally through the full rotation – allowing for smooth transitions of foil angles, while still capturing some of the advantages of keeping α in the maximum lift range. One example of articulation can be seen in Figure 1.

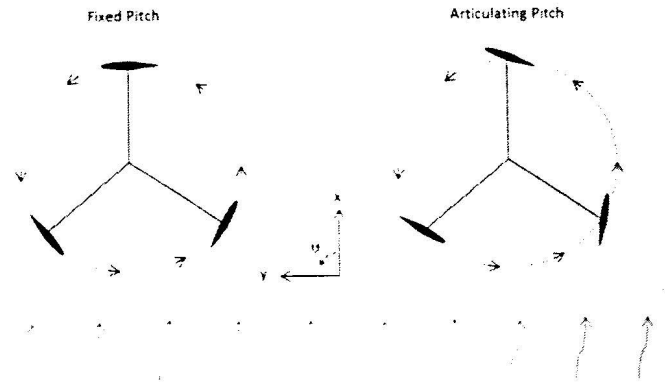


Figure 1: Top view of VAWTs showing articulating pitch

METHODS

The Model Structure

While the field of dynamic modeling of wind turbines has advanced considerably in the past 20 years, the bulk of the research has been focused on commercial-scale horizontal axis turbines (HAWT)'s [10]. Models tend to fall into one of two categories: those that deal with the details of the flows and forces around the rotor and the wakes downstream, and those that deal with the structural and dynamic response of the mechanical structure and power train. While it's possible to combine the two approaches, it is rarely done due to the fact that the computational load brought about by the Computational Fluid Dynamics is quite high compared to the modest load imposed by the lumped parameter power and drivetrain model. In addition, the two models are generally interested in different results. The former is used for detailed blade and rotor design and for studying the effects of downstream wakes on other turbines in an array, while the latter is interested in the dynamic response of the generator to changes in wind speed as well as the structural loading on the mechanical components in the nacelle. Finally, we point out that the fluid flow and subsequent wakes in a VAWT are fundamentally different and, in some ways, much more complicated as the rotor elements on the down-wind arc of the rotor are passing through the wake of the elements of the upstream arc.

This paper presents a model that is an extension to others found in the literature in which the aerodynamic model is quasi-static using the published lift and drag coefficients of known airfoils. This approach has been proven to be effective in capturing the energy capture of VAWTs so that the drivetrain behavior and power capture can be studied [11-13].

The result of this research is a model implemented in MATLAB¹ and Simulink. The general structure of the model can be seen in Figure 2. The dynamic state variables of the model are simply the rotor rotational velocity and position and are defined in the central block of the model. The rotor speed is

¹ MATLAB is a product of MathWorks Inc.

used to compute the electrical output through a simple algebraic generator/load model.

As will be shown in greater detail, the bulk of the model makes use of coordinate transformations and vector operations to find the instantaneous lift and drag forces on each vertical airfoil as a function of wind speed, rotor velocity, rotor position, generator current and generator power output.

The last variable is important in that it is used to compute the induction factor, which accounts for the fact that the air speed is reduced as it passes through the VAWT volume as some of the kinetic energy of the wind is converted to useful power.

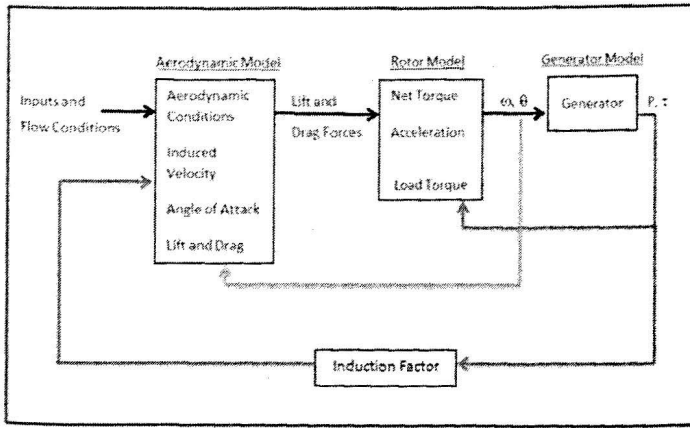


Figure 2: General flow diagram of the model

Aerodynamic Conditions

The aerodynamic conditions consist of the fluid properties, the airfoil lift and drag properties, and the inertia of the system. The fluid properties were defined for air at standard ambient temperature and atmospheric pressure (25 °C and 100 kPa) and included the velocity and density of the flow, and the viscosity.

The lift and drag properties were based on experimental results from a wind-tunnel at Sandia National Lab [14]. Two symmetrical airfoils were used in the analysis: NACA 0015 and NACA 0018. The lift and drag coefficients were listed for 11 different Reynolds numbers between 10,000 and 10,000,000. The lift and drag coefficients were provided for 119 different angles of attack between 0° and 180°. The values are mirrored from 180° to 360°. Linear interpolation was used to compute specific lift and drag properties for any angle and any Reynolds number within that range.

The input fluid velocity is given in three different vector components: U_x , U_y , and U_z . For most simulations U_y and U_z were left at zero. The input for U_x is not the free-stream velocity (which was usually a constant), but instead is an average of the upstream and downstream velocities.

$$U_x = \frac{U_1 + U_2}{2} \quad (1)$$

The free-stream velocity and the downstream velocities are different, because some of the kinetic energy from the stream is transferred to the rotation of the turbine, which, in turn, is extracted in the form of electrical power at the generator. The flow velocity experienced by the leading foil of the turbine is approximately equal to the free-stream velocity, while the flow velocity experienced at the downstream foil is approximately equal to the downstream velocity. This variation is modeled using an induction factor.

The induction factor is a ratio of the fluid velocity upstream of a turbine to the fluid velocity downstream of the turbine. The more energy is extracted from the flow by the turbine, the more the flow downstream of the turbine will slow. As such, the induction factor can also function as the ratio of the turbine power to the power in the fluid flow [10]. This factor (symbolized by the letter a) is a function of the coefficient of power of the turbine (2).

$$C_p = 4a(1-a)^2 \quad (2)$$

It is best to understand the induction factor by considering the effect of changing generator loading. If the generator is unloaded, the power extracted is zero and both C_p and a are zero. As the generator is gradually loaded, both C_p and a increase to a maximum value when $a = 1/3$. Increased loading will decrease the turbine performance beyond its effective range, decreasing overall energy production. The coefficient of power was calculated using a MATLAB function based on equation (3).

$$C_p = \frac{P}{\frac{1}{2} \rho A U^3} \quad (3)$$

This was the value of the coefficient of power that was incorporated into the interpolation function that determined the induction factor, a . The induction factor allowed one to determine the downstream fluid velocity based on the upstream velocity as shown in (4).

$$U_2 = a \cdot U_1 \quad (4)$$

Combining equations (4) and (1) gave the value of U_x based on the induction factor. The same process would be applied for any velocity in the y direction, but for the simulations performed in this study, the value of U_y was left at 0, otherwise induction would apply to U_y as well. The value of U_x was used to then compute the flow conditions that lead to the calculation of the torque.

Rigid Body Dynamics

The equations of motion consist of a series of coordinate transformations represented as matrices. There were three transformations from the global position of the rotor to the individual angle of each foil and are displayed in Figure 3.

The first set of axes (called Frame Z) is a fixed, global frame that defines the axis of rotation of the rotor about the (upward pointing) z-axis in terms of an angle θ (Theta). The second frame (A) rotates with the rotor. It shares the same z-axis as frame Z, but its x-axis is rotated by θ from the x-axis in Z. Frame B is translated out to the foil itself where its y axis is tangent to the circle of rotation. Frame B shares the same direction for x as frame A, but its z-axis is offset from frames Z and A by a distance of R, the turbine's radius. The foil coordinate frame (C) shares the z-axis of frame B, but is rotated so that its x-axis is in line with the chord of the foil. The pitch of the blade, described by ψ , is the angle between the y-axis of the B-frame and the x-axis of the C-frame.

When air passes through a turbine, the two aerodynamic forces of lift and drag develop on each foil. These two forces are at orthogonal angles to one another – with the drag being parallel to the relative velocity at each foil. By calculating the net force at each foil (the sum of the lift and drag forces) one can calculate the net effect of the aerodynamic forces at work.

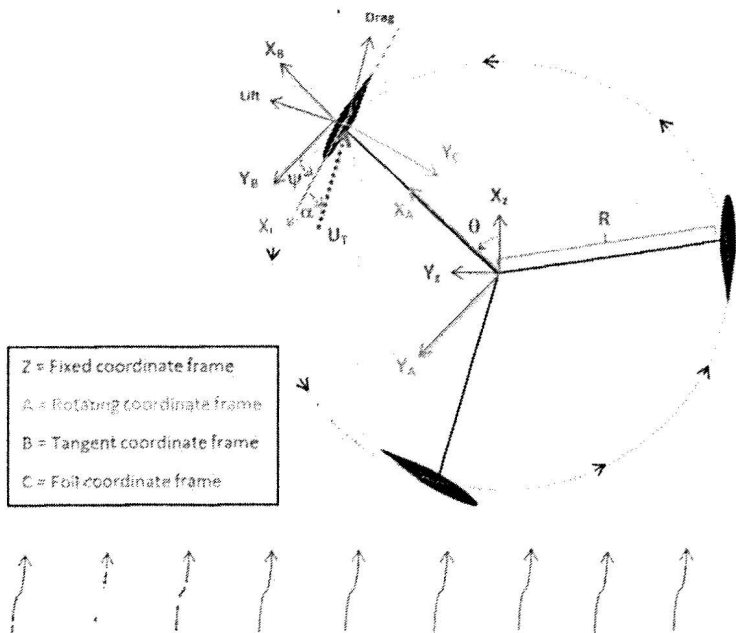


Figure 3: The four coordinate frames used in the model

Once the turbine begins rotating, the relative velocity experienced at each foil is affected by the so-called induced wind due to the rotational velocity of the rotor. This changes the relative fluid velocity and the resulting lift and drag forces both in terms of magnitude and direction. The relative velocity at each foil can be determined using the principles of vector addition to account for both the free-stream velocity and the velocity of the foil.

The resultant velocity at each air foil is referred to as the relative velocity because it is different for each foil of the turbine. The rotation of the turbine alters the angle of resultant velocity to a direction that more closely resembles the circular arrangement of the rotor's circumference. This decreases α , increases the lift, and allows the turbine to spin up rapidly into a regime where power production can begin.

Calculating Torque

The geometric transformations allow the position of the foil to be calculated at any instant. Assuming that the axis of the VAWT is the upward-pointing z-axis (Frame Z), the flow experienced in the x-direction is the sum of the free-stream flow in the x-direction, and the x-aspect of rotational velocity. The flow experienced in the y-direction is the difference of the free-stream flow in the y-direction and the y-aspect of rotational velocity. These components are shown in Figure 4.

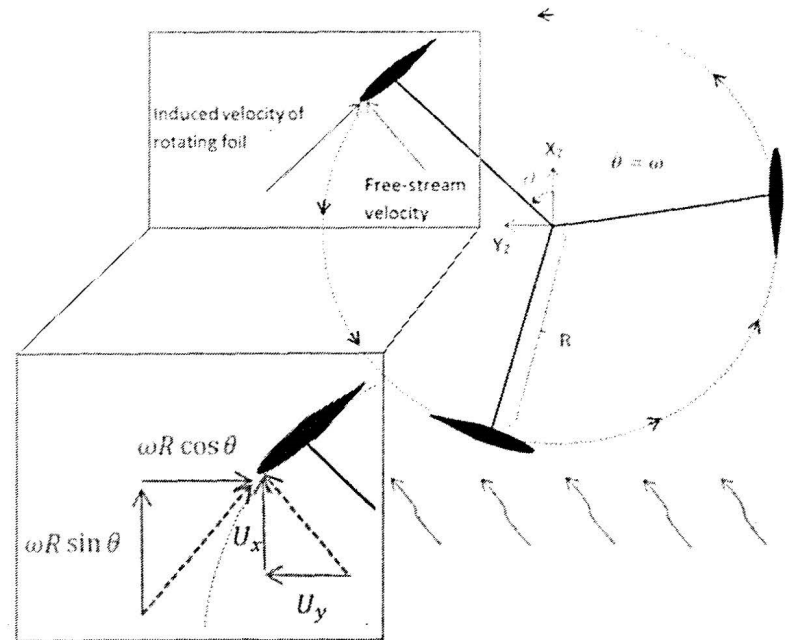


Figure 4: Vector components of velocities at a foil

By adding each of the directional components together, one can find the resultant, or relative velocity at each foil. The relative velocity vector, U_T is described by the following mathematical breakdown of the three dimensional vector in the global coordinate system (Frame Z).

$${}^Z U_T = ({}^Z U_x + \omega R \sin \theta) \hat{i} + ({}^Z U_y - \omega R \cos \theta) \hat{j} + ({}^Z U_z) \hat{k} \quad (4)$$

In order to transform this vector from the global coordinate frame system to the axes at the foil, the three elements of ${}^Z U_T$ are multiplied by the transformation matrix ${}^Z \Pi_C$ to account for the orientation and pitch of the foil. The pitch is given by the value of ψ which is the angular difference between the chord

of the foil and the line tangent to the perimeter of rotation at that position (see Figure 3). The transformation of the total relative velocity from the global frame to the foil frame is shown in equation (5).

$${}^Z\Pi_C \times {}^ZU_T = {}^CU_T$$

$$\begin{bmatrix} -\sin(\theta + \psi) & \cos(\theta + \psi) & 0 & R \sin \theta \\ -\cos(\theta + \psi) & -\sin(\theta + \psi) & 0 & R \cos \theta \\ 0 & 0 & 1 & 0 \\ 0 & 0 & 0 & 1 \end{bmatrix} \times \begin{bmatrix} U_{Tx} \\ U_{Ty} \\ U_{Tz} \\ 0 \end{bmatrix} = \begin{bmatrix} U_{Tx} \\ U_{Ty} \\ U_{Tz} \\ 0 \end{bmatrix} \quad (5)$$

The resulting vector, CU_T describes the relative velocity in terms of the axes aligned with the foil that includes the pitch of the foil. Once the direction of the relative velocity is understood in relation to the axes at the foil, the angle of attack can be computed as shown in (6).

$$\alpha = \tan^{-1} \frac{{}^CU_{Ty}}{{}^CU_{Tx}} \quad (6)$$

While the direction of the relative velocity is known by U_T its magnitude is computed as shown in (7).

$$U_{tot} = \sqrt{({}^ZU_{Tx})^2 + ({}^ZU_{Ty})^2} \quad (7)$$

The total flow velocity in addition to the fluid properties allows one to compute the Reynolds number.

$$Re = \frac{\rho U_{tot} C}{\mu} \quad (8)$$

Knowing α and the Reynolds number, the coefficients of lift and drag (C_l and C_d) were interpolated from a table of values from previous experimental results [14]. The lift and drag forces were computed using equations (9) and (10).

$$L = \frac{1}{2} \cdot C_l \cdot \rho \cdot U_{tot}^2 \cdot C \cdot H \quad (9)$$

$$D = \frac{1}{2} \cdot C_d \cdot \rho \cdot U_{tot}^2 \cdot C \cdot H \quad (10)$$

The resulting torque from the lift and drag is calculated using matrix transformations to transform the forces on the rotating foil to the fixed center of rotation by the transform shown in equation (11).

$${}^C\Pi_Z = \begin{bmatrix} \cos(\theta + \frac{\pi}{2} + \psi) & -\sin(\theta + \frac{\pi}{2} + \psi) & 0 & -R \cos \theta \\ \sin(\theta + \frac{\pi}{2} + \psi) & \cos(\theta + \frac{\pi}{2} + \psi) & 0 & R \sin \theta \\ 0 & 0 & 1 & 0 \\ 0 & 0 & 0 & 1 \end{bmatrix} \quad (11)$$

The transformation matrix allows for the communication between the forces at the foil, and the conditions at the fixed center of rotation. The drag force was defined as working in the positive x direction and the lift force working in the positive y direction. The distance from the center of rotation was defined as R as shown in (12).

$$R = \begin{bmatrix} R \cos \theta \\ R \sin \theta \\ 0 \\ 1 \end{bmatrix} \quad (12) \quad F = \begin{bmatrix} D \\ L \\ 0 \\ 0 \end{bmatrix} \quad (13)$$

The torque then becomes a product of these three matrices as shown in equation (14).

$$\tau = R \times {}^C\Pi_Z \times F \quad (14)$$

This matrix multiplication simplifies down to a single equation (15).

$$\tau = R \cdot L \cdot \sin(\psi + \alpha) - R \cdot D \cdot \cos(\psi + \alpha) \quad (15)$$

The power output of the turbine is modeled as a simple DC generator with a resistive load, the torque due to the generator being proportional to the rotational velocity (16).

$$\tau_{Gen} = r \cdot \omega \quad (16)$$

Increasing or decreasing the value of r has the same effect as increasing or decreasing the load of a generator. The power output of the system is the product of the generator load and the rotational velocity, ω .

$$P = \tau_{Gen} \cdot \omega \quad (17)$$

The resultant torque on the shaft, τ_{net} , is the difference between the aerodynamic torque from each foil and the generator torque. This is the input torque given to the "Joint Actuator" block that is part of the rigid body dynamics of the system.

$$\tau_{net} = \tau_{foil1} + \tau_{foil2} + \tau_{foil3} - \tau_{Gen} \quad (18)$$

RESULTS

Start-up Behavior

Once the turbine model was developed, the simulation results of the running model were compared to the empirical data from other studies. One such test was performed at Durham University in which a three-bladed Darrieus VAWT was set up in a wind tunnel. The rotor was attached to a three-phase permanent magnet generator with a rating of 200W [8]. Although no power measurements were reported in the wind-tunnel tests, the acceleration and rotational behavior of the turbine in the wind-tunnel provided a basis for qualitative evaluation of the simulation model. In the wind tunnel, the turbine went through a period of slow rotation before a sudden increase in rotational velocity that leveled out at a high TSR of above 3. This was the same behavior evidenced in the simulations of MATLAB model.

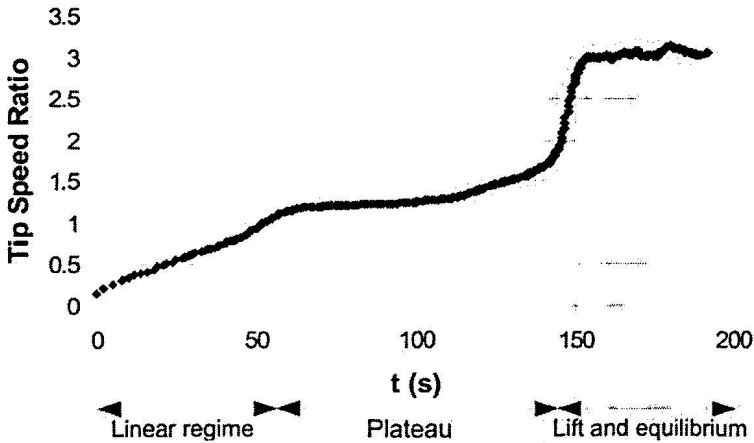


Figure 5: Results of a wind-tunnel test of a fixed-pitch 3-Bladed VAWT at wind-speed of 6m/s. Words and figure from [8]

The simulation showed qualitatively similar responses to that shown in Figure 5. It was discovered however that higher generator loads prevented the ultimate acceleration to higher TSR values and the speed would plateau just under a TSR of 1. When the generator load was reduced to a low enough value, the turbine would accelerate to a TSR of close to 1 for a while, and then suddenly transition to a very high rotational speed of up to 7 TSR and much higher power coefficients.

Pitch Articulation

Pitch articulation is defined in equation (19) where the pitch, ψ , varies sinusoidally with θ , where $\theta = 0$ corresponds to the downwind direction.

$$\psi = M \cdot \cos \theta \quad (19)$$

When sinusoidal pitch articulation was added, a consistent trend emerged with a steady state of rotation occurring at a TSR near 3.5.

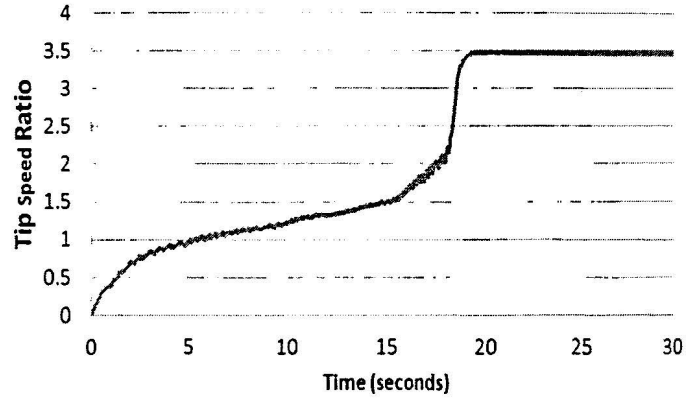


Figure 6: Simulation of VAWT speed up from rest sinusoidally varying pitch at a wind speed of 7m/s

The sinusoidal articulation limited the angle of attack that was experienced at each foil. For NACA 00xx foils, peak C_l is achieved near $\alpha = 14^\circ$ a stall occurs near $\alpha = 20^\circ$. The variable-pitch model avoids this regime by keeping a small, whereas almost a full range of α is experienced for the fixed pitch turbine. Figure 7 shows a plot of α vs. angle of rotation as predicted by the simulation. The data plotted were extracted from the simulation after a steady-state (near constant velocity) was achieved. The figure contrasts the large changes in the angle of attack experienced by fixed pitch machines with the nearly constant angle of attack achieved by articulating the pitch.

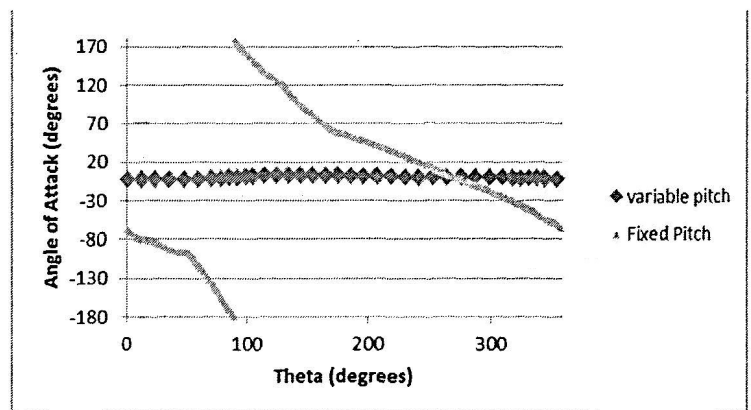


Figure 7: Angle of Attack vs. rotor rotation angle for a VAWT at constant speed with articulating and fixed foils (pitch articulation magnitude = 9°).

The variable pitch model has a much narrower range of α , with subsequently higher coefficients of lift than the fixed-pitch turbine. While it's not clear that a simple sinusoidal pitch function will keep the angle of attack at an optimum, it is clear from Figure 7 that stalling (which clearly occurs for fixed-pitch foils) can be avoided throughout the rotation.

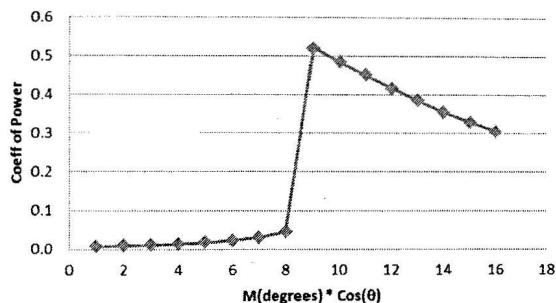


Figure 8: Coefficient of Power (C_p) as a function of angle articulation magnitude at a nominal wind speed of 8 m/s.

Figure 8 shows the results of simulations of a VAWT model with varying magnitudes of sinusoidal pitch variation. This function had a maximum positive pitch deflection (outward from the circle of rotation) occurring on the windward point of rotation and negative deflection (inwards toward the center of rotation) on the leeward point. A large change occurs between a magnitude of eight and nine degrees. The reason for this discontinuity is because once the pitch amplitude reached a value greater than eight degrees, the turbine was able to reach high TSRs changing the range in α . Further investigation at more detail showed the ideal magnitude to be a value of 8.6° .

The dramatic difference in performance between an articulating and a fixed-pitch VAWT is shown in Figure 9. Based on the same model as that of Figure 6, Figure 9 illustrates that the articulation of the foils provides significantly more torque to the rotor because of higher lift coefficients. At wind-speeds lower than 10m/s, the fixed pitch model would barely rotate at all. The result was a power output that was 2 orders of magnitude greater for the sinusoidally pitching foils compared to fixed-pitch foils. For example, at 10 m/s wind speed, the simulation predicted only 13 Watts output for the fixed pitch rotor, but 1900 Watts for the sinusoidally varying pitch.

The Darrieus VAWT with symmetric foils allowed for better operation at low wind-speeds than similar VAWTs that had only fixed-pitch foils. This is similar to the conclusion reached by an experimental study based on H-Darrieus VAWTs with symmetric foils that found “the best performance is achieved at pitch angle about 8° ” [15]. Another study came to a more general conclusion that “the amplitude of the sinusoidal correction function is set equal to the maximum difference between the local geometric angle of attack and the blade static stall angle” [9] which is a sinusoidal function varying in amplitude by approximately 11° .

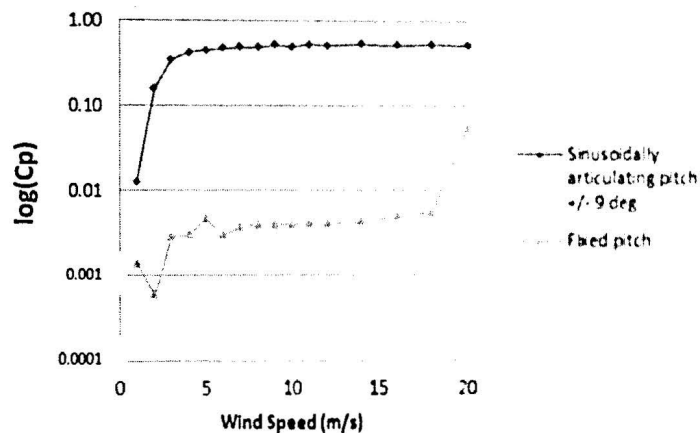


Figure 9: Log of power coefficient vs wind speed for fixed pitch and variable pitch VAWTs

Dynamic Generator Loading

The model demonstrated the effectiveness of having a dynamic generator load that could change according to differences in the flow conditions. Having a low generator load at start-up allowed the turbine model to begin rotating from rest. Minimizing the generator load for low wind velocities allowed the turbine to reach high TSRs, reducing the angle of attack and increasing lift. Once the turbine reached a $TSR > 1.5$, the power output could be improved by slowly increasing the generator load even though this decreased the rotor’s rotational speed. Overloading the generator caused the model turbine to go into a stall condition and it would rapidly decelerate. Too great of a generator load in the initial stages of the simulation would prevent the turbine from spinning at all. However, the danger does remain of having a turbine under-loaded at high velocity conditions. Rotational speeds greater than 200 RPM had the possibility of compromising the materials and structure of the turbine – a problem that can be solved either with a more conservative loading scheme or constructing a machine out of higher strength materials that could manage the tensile and bending stresses of high rotation. Three graphs are shown below of MATLAB simulations at a wind-speed of 9 m/s that demonstrate the effects of increasing the load on a turbine until stall is reached.

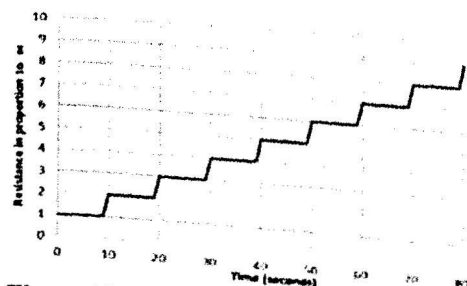


Figure 10: Simulated load profile for VAWT generator

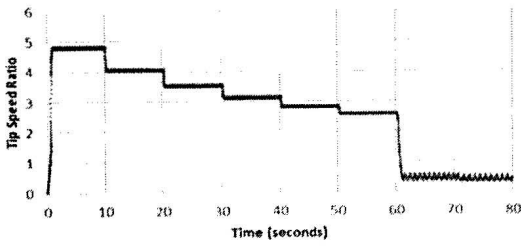


Figure 11: Simulation results of TSR response to increasing generator load

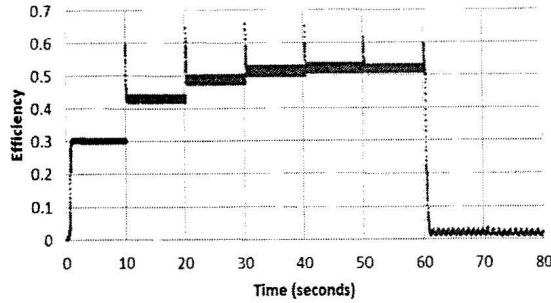


Figure 12: Simulation results of C_p response to increasing generator load

As one can see from Figure 12, increasing the generator load has a significantly beneficial impact on the power production for the first several steps. The increased torque on the generator reduces the rotational speed but still increases the power output to a certain point. However, with each subsequent load increase there is a smaller effect on the power, and the turbine becomes less rotationally stable. Eventually, the lift forces acting on the turbine are not great enough to continue turning the rotor. The turbine loses speed, and in doing so, the induced velocity of each rotation is very small with large angles of attack. This combined with a high resistive torque causes the turbine to reach a stall condition. While this is better than a turbine self-destructing from high rotational speeds, it has an adverse effect on the power production of the turbine.

Comparison with Field Data

The main purpose of this study was to develop a simulation which could be used to improve the design and operation of a specific VAWT concept, the Blackhawk [7]. During May, 2011, a prototype turbine was deployed in Emmet, Idaho and its performance monitored. Figure 11 shows the power produced by the turbine as a function of the measured wind speed. The output predicted by the simulation is plotted on the same graph.

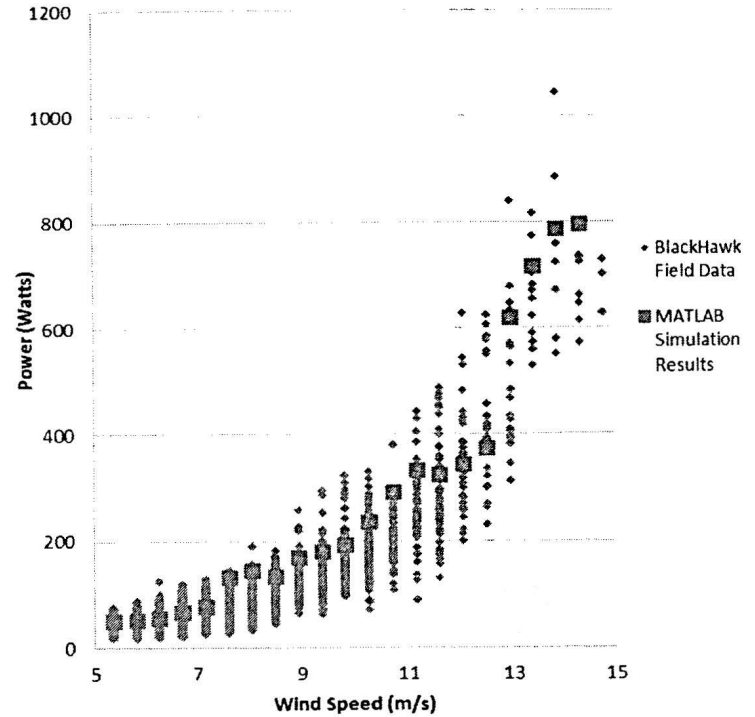


Figure 11: Power output vs. wind speed for prototype Blackhawk deployment and predicted output.

CONCLUSIONS

The purpose of the study was to analyze the dynamic behavior of an innovated Vertical Axis Wind Turbine design for Darrieus-style turbines with foils that articulate with a prescribed behavior as the foil rotates around the axis. The model, implemented in MATLAB/Simulink, utilizes a fairly simple quasi-steady state aerodynamic approach which results in a relatively low-order model that lends itself to design studies and optimization.

Validation was attempted by comparing the model behavior with fixed-pitch foils to empirical studies for similarly designed turbines. The model results compare favorably to those data, particularly in the complex behavior observed as the turbine starts from rest. Published results indicated that this class of turbines progress through various distinct phases of operation, starting with a slow startup phase, moving to a prolonged plateau of fairly low TSR. If conditions are right, the turbine may then make a sudden shift to much higher rotational speeds, with TSR's near 3 or 4. It is in this higher speed domain that the turbines find their highest performance as measured by power production.

When the model was expanded to include articulated foils (pitch as a function of rotational angle), the model confirmed that articulation can lead to greatly improved performance, particularly in the lower-wind regime. In some cases, a 2 order-of-magnitude improvement in energy

production was observed. Additionally, it was shown that the relationship between performance and pitch magnitude can be highly sensitive with potential for discontinuities in the relationship. This has implications for design and optimization of a turbine which will see a wide range of operating conditions. This relationship needs to be explored further.

The model with articulating foils also exhibited the characteristic, three-phase startup behavior which could achieve fairly high TSR's and high energy conversion rates.

Startup behavior was also examined using the model. The model with fixed pitch foils exhibits the well-documented problems of starting from rest in a moderate to high wind. In most simulations, the rotor tended to oscillate between two rotor positions as the foils reacted to the wind (with no induced wind due to the rotation). And, as was also reported in the literature, the model with articulated foils was able to reliably start from rest in a moderate wind.

Finally, the role of dynamic generator control was explored. We found that the high TSR regime (in which the turbines experienced superior performance) can be reliably achieved by starting with an unloaded generator and gradually ramping up the load (and hence, the energy extraction) as the turbine comes up to speed. It is clear that the interaction between wind speed, rotor rotational velocity, foil pitch and generator load is a rich and complex design space which models such as this can be used to further explore.

Now that the model has been developed, it can be used to test new turbine designs and configurations. While some exploration was done on the effects of periodic and sinusoidal pitch articulation, there is much more that could be studied on the subject, such as optimizing the angle of attack for maximum lift for specific models and configurations of VAWTs. The model itself could be further refined by accounting for friction in the bearings and the effects of turbulence on the foils. Additionally, more could be done to better define the foil-to-foil interaction and the wake effects on the foils during rotation. The model used data based on two-dimensional flow, and ignored span-wise flow or flow in the Z-direction.

REFERENCES

- [1] World Wind Energy Association, "World Wind Energy Report 2010," World Wind Energy Association, Bonn, Germany, 2011.
- [2] National Renewable Energy Laboratory, "20% Wind Energy by 2030: Increasing Wind Energy's Contribution to the U.S. Electric Supply," Department of Energy, Oak Ridge, 2008.
- [3] Energy Information Administration, "Annual Energy Review 2011," U.S. Energy Information Administration, Washington DC, 2012.
- [4] U.S. Department of Energy and the American Wind Energy Association, "Vertical Axis Wind Turbines: The History of the DOE Program," Sandia National Laboratories, Albuquerque.
- [5] H. Riegler, "HAWT versus VAWT: Small VAWTs Find a Clear Niche," *Refocus*, pp. 44-46, July/August 2003.
- [6] K. Pope, I. Diner and G. Naterer, "Energy and Exergy Efficiency Comparison of Horizontal and Vertical Axis Wind Turbines," *Renewable Energy*, vol. 35, pp. 2102-2113, 2010.
- [7] B. Boatner, "Vertical Axis Wind Turbine With Articulating Rotor". United States of America Patent 7,677,862, 2 March 2010.
- [8] H. Hill, R. Dominy, G. Ingram and J. Dominy, "The Physics of Self-Starting," in *Institute of Mechanical Engineers, PartA: journal of power and energy*, 2009.
- [9] Y. Staelens, F. Saeed and P. I., "A Straight-Bladed Variable-Pitch VAWT Concept for Improved Power Generation," in *ASME Wind Energy Symposium*, Reno, 2003.
- [10] C. Lynch, *Advanced CFD Methods for Turbine Analysis*, Atlanta, GA: PhD Dissertation, Department of Aerospace Engineering, Georgia Institute of Technology, May, 2011.
- [11] M. Hansen, A. Hansen, L. Torben, S. Oye, P. Sorenson and P. Fuglsang, "Control Design for a Pitch-Regulated, Variable Speed Wind Turbine," Riso National Laboratory, Roskilde, 2005.
- [12] O. Guerri, A. Sakout and K. Bouhadef, "Simulations of the Fluid Flow around a rotating Vertical Axis Wind Turbine," *Wind Engineering*, vol. 31, no. 3, pp. 149-163, 2007.
- [13] M. Islam, D.-K. Ting and A. Fartaj, "Aerodynamic Models for Darrieus-Type Straight-Bladed Vertical Axis Wind Turbines," *Renewable and Sustainable Energy Reviews*, vol. 12, pp. 1087-1109, 2006.
- [14] R. Sheldahl and P. Klimas, "Aerodynamic Characteristics of Seven Symmetrical Airfoil Sections through 180-Degree Angle of Attack for Use in Aerodynamic Analysis of Vertical Axis Wind Turbines," Sandia National Laboratory, Albuquerque, 1981.
- [15] M. El-Samanoudy, A. Ghorab and S. Youssef, "Effect of Some Design Parameters on the Performance of a Giromill Vertical Axis Wind Turbine," *Ain Shams Engineering Journal*, vol. 1, no. 1, pp. 85-95, 2010.